




High capacitive Pt and NiO_x loaded supercapacitors with commercial and green synthesized carbon-based materials

Serkan Demirel¹, Mehmet Salih Nas^{2,5}, Adem Kocyigit^{3,*} , Mehmet Harbi Calimli^{4,5}, and Mehmet Hakkı Alma⁵

¹ Department of Electricity and Energy, Iğdir University, 76000 Iğdir, Turkey

² Department of Environmental Engineering, Faculty of Engineering, Iğdir University, 76000 Iğdir, Turkey

³ Department of Electronics and Automation, Vocational High School, Bilecik Şeyh Edeballı University, 11000 Bilecik, Turkey

⁴ Department of Medical Services and Techniques, Tuzluca Vocational School, Iğdir University, 76000 Iğdir, Turkey

⁵ Research Application Laboratory and Research Center (ALUM), Iğdir University, Iğdir, Turkey

Received: 24 August 2023

Accepted: 21 December 2023

Published online:
18 January 2024

© The Author(s), 2024

ABSTRACT

Supercapacitors have gained great interest due to their high-power energy density, suitability for clean energy and energy storage applications. In this study, we used commercial multi-walled carbon nanotube (MWCNT), polypyrrole (PPy) and synthesized porous carbon (PC) from *Astragalus brachycalyx* plant as supporting materials to prepare Pt-NiO_x/PPy-MWCNT and Pt-NiO_x/PC electrodes by a straightforward method and tested their electrochemical properties for supercapacitor applications. X-ray diffractometer (XRD), scanning electron microscope (SEM) and energy dispersive spectroscopy (EDS) were employed to characterize synthesized electrodes. The XRD results confirmed the composition and crystalline structure of related materials in the Pt-NiO_x/PPy-MWCNT and Pt-NiO_x/PC electrodes. While the MWCNT supporting materials with PPy exhibited filled rod like structure, PC supporting materials showed porous surfaces according to SEM images. The EDS analysis approved chemical composition of the Pt-NiO_x/PPy-MWCNT and Pt-NiO_x/PC depending on their ingredients. Cyclic voltammetry (CV) measurements were used to characterize capacitor behaviors of the electrode materials in a Swagelok-type cell. The Pt-NiO_x/PPy-MWCNT and Pt-NiO_x/PC materials displayed 252.36 F/g and 390.97 F/g capacitance values, respectively. The electrochemical experiments revealed that the synthesized materials can be used as energy storage electrode materials for supercapacitor applications.

Address correspondence to E-mail: adem.kocyigit@bilecik.edu.tr

1 Introduction

The use of clean energy is vital for sustainable development in today's society, and one of another important issue is to storage energy, which can be made by supercapacitors, in natural ways [1–3]. Supercapacitors are known as a double-layer electric capacitors, and they have many advantages such as long cycle life, high power and energy density, fast charge and discharge, friendly to the environment and low cost [4–6]. Due to these advantages, they have gained great interest in the field of energy storage, and can be widely used in many electrical applications such as emergency backup powers, electric-vehicles, medical area, airbags, power-banks etc. [7, 8]. Researchers have studied on electrode, binders, current collectors, electrolyte materials, and separator of supercapacitors [9]. Various materials and optimization techniques are widely used to improve supercapacitor performance by using various electrode materials for high chemical stability and wide specific surface area [10]. For example, activated carbon (AC), carbon nanotubes (CN), polyaniline (PANI), polypyrrole (PPy), multi-walled carbon nanotubes (MWCNT) are some of the materials that used as support in the preparation of various supercapacitors [11, 12]. While the reactions take place both on the electrodes and in electrolytes, the charge/discharge events occur only on the electrodes in supercapacitors, and thus the material of electrodes and electrolytes is very important due to impact on the supercapacitor performance [13, 14]. Carbon-based materials have been employed in supercapacitor applications as electrodes after eliminating deficiencies by using some metal and polymer materials [15, 16]. Many researchers have developed composite materials such as mixed metals and polymers to improve performance of cyclic stability and specific capacitance in supercapacitors [17–22]. As a carbon-based material, MWCNT makes a significant contribution to improvement of mechanical properties by increasing the stability of the formed composite structure, and it provides to increase conductivity properties of materials without changing the electronic structure [20, 23]. Furthermore, successful studies have been carried out by using various noble metals like Pd, Ru, etc. with and without MWCNT to increase electronic activity for non-enzymatic H_2O_2 sensors [24, 25]. Addition of Pt metal particles into carbon-based materials can increase supercapacitor power density of electrode materials and decrease power/

charge transfer resistance [26]. Moreover, several carbon-based materials like polypyrrole (PPy) have been used for preparation and tuning of electrode materials with carbon-based materials in the composition, and this has been detected to be effective way to increase of the supercapacitor performance [27–29]. In addition, porous carbon (PC) derived by green synthesis have been widely used in supercapacitor electrodes for energy storage materials due to their high surface area and porous structure [30, 31]. The PC has been used in double-layer capacitors and pseudocapacitors according to the adsorption-desorption mechanism formed on their surfaces [32–34].

Most of carbon sources such as MWNCT, PPy are available commercially market. However, to use green synthesized carbon sources can protect environment, and may cheaper than commercial ones with same performance applications. Aim of this study is to synthesize high performance carbon-based electrode materials by green synthesis method for supercapacitor applications. In that aim, we used commercial MWCNT with PPy and green synthesized PC as supporting material for loading of Pt and NiO. Thus, Pt-NiO_x/PPy-MWCNT and Pt-NiO_x/PC materials have been obtained, and their electrochemical properties tested as supercapacitors.

2 Materials and methods

2.1 Chemicals

Precursors of PtCl₂, cetyltrimethylammonium bromide (CTAB), nickel (II) chloride, palladium (II) chloride, sodium borohydride (NaBH₄), MWCNT, and polypyrrole (PPy) were purchased from Sigma with analytical degree and employed directly without any purification process. Hydrochloric acid (HCl) and sulfuric acid (H₂SO₄) were supplied from Merck.

2.2 Synthesis porous carbon (PC) derived from *Astragalus brachycalyx* plant

Astragalus brachycalyx plants were collected in a mountainous region of Hakkari City, in Turkey. *Astragalus brachycalyx* plant firstly was dried in a dark environment at 78 °C for 48, and then were ground and sieved, and then PC was prepared by carbonization process for treated *Astragalus brachycalyx* plant at a pyrolysis device under nitrogen atmosphere of 5 °C/min at

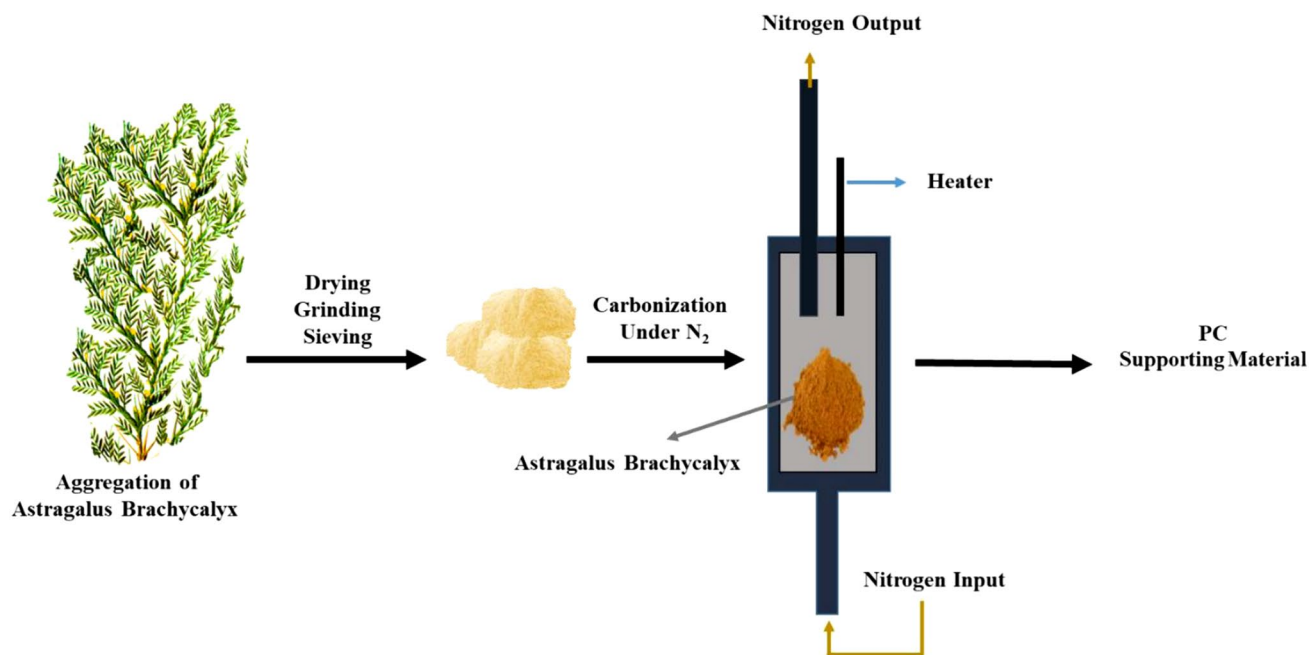


Fig. 1 Production procedure of the PC supporting material

600 °C for 1 h. The obtained carbonized materials were washed with distilled water and dried in an oven at 105 °C for 24 h [35]. Schematic illustration of the production of the PC has been shown in Fig. 1.

2.3 Synthesis of Pt-NiO_x/PPy-MWCNT materials

MWCNT/PPy nanomaterial was prepared by the interaction of MWCNT suspension solution and oxidative polymerization of pyrrole monomer. MWCNT (0.50 g) was added into a 40 ml water in a vessel and kept in the sonication medium for 30 min. Then, CTAB (0.15 g), hydrochloric acid (120 mL) and pyrrole (0.30 mL) materials were added into the mixture, and the mixture was stirred for 12 h to form the pyrrole monomer structure surrounded by MWCNT. In another vessel, a new solution was prepared by dissolving 3 g ammonium persulfate (APS) in hydrochloric acid (5 M, 200 mL). This prepared solution was added dropwise into the pyrrole monomer solution integrated with the MWCNT suspension by a smart pipette. The stirring of the final solution was kept in the ice bath for about 60 min and then allowed to polymerize at about 6 h at room temperature conditions. The resulting MWCNT/PPy precipitate was centrifuged and washed with distilled water and ethanol to remove unwanted impurities. The final product was left to dry in a vacuum

oven at 75 °C [36, 37]. The synthesized PPy/MWCNT (1 g) powder was homogeneously dissolved in 200 mL water by an ultrasonic bath for 30 min. PtCl₂ (177 mg, 10 m M) was added into this mixture and stirred for an additional 30 min. Then, NaBH₄ (750 mg, 20mM) as a reducing agent was added into the solution medium and stirred for 1 more hour. The final solution was filtered by a filter, and obtained product was washed profusely by distilled water and methanol. It was dried in a vacuum oven at 80 °C for 12 h at the end. For a better understanding, the synthesis protocols of the Pt-NiO_x/PPy-MWCNT materials have been summarized in Fig. 2 as schematically.

2.4 Synthesis of Pt-NiO_x/PC materials

Typically, Pt-NiO_x/PC was synthesized using the chemical reduction method combined with the easy-impregnation technique. Firstly, the Na₂PtCl₄ precursor solution was obtained by adding PtCl₂ into aqueous NaCl solution. Then, 1.1 mL of Na₂PtCl₄ and 0.0550 mL of NiCl₂ were added into 4.60 mL of DI water and mixed for 10 min. Then, 100 mg of PC was added into the solution medium, and the mixture was kept in the ultrasonic environment for 1 h to ensure dispersion homogeneously. A 0.5 mL of NaOH solution was added into the resulting suspension and mixed for 30 min. 42 mg of NaBH₄ was also added to

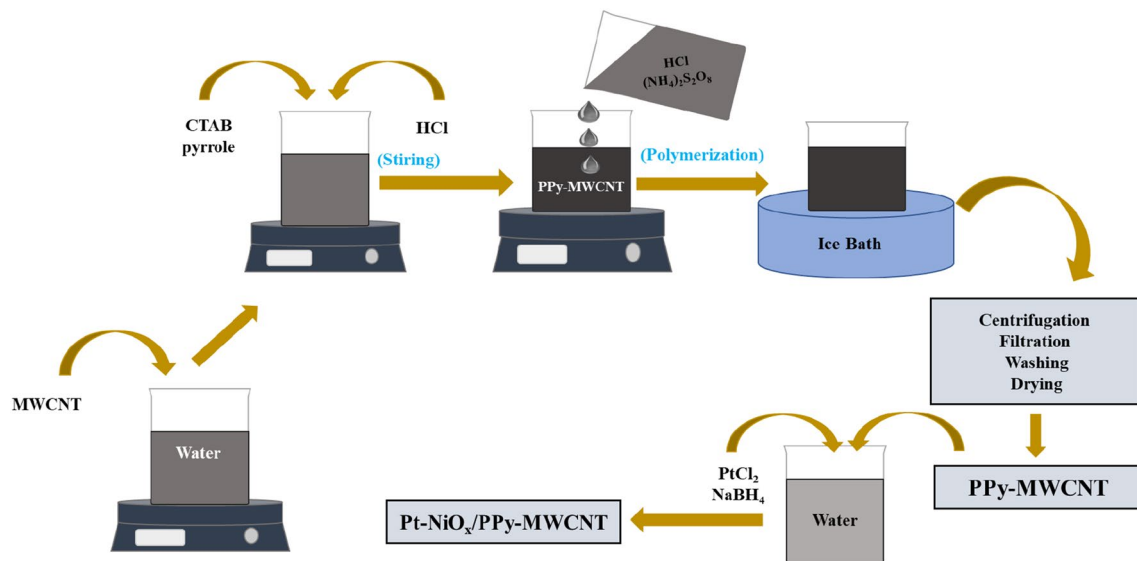


Fig. 2 Production procedure of the Pt-NiO_x/PPy-MWCNT electrode materials

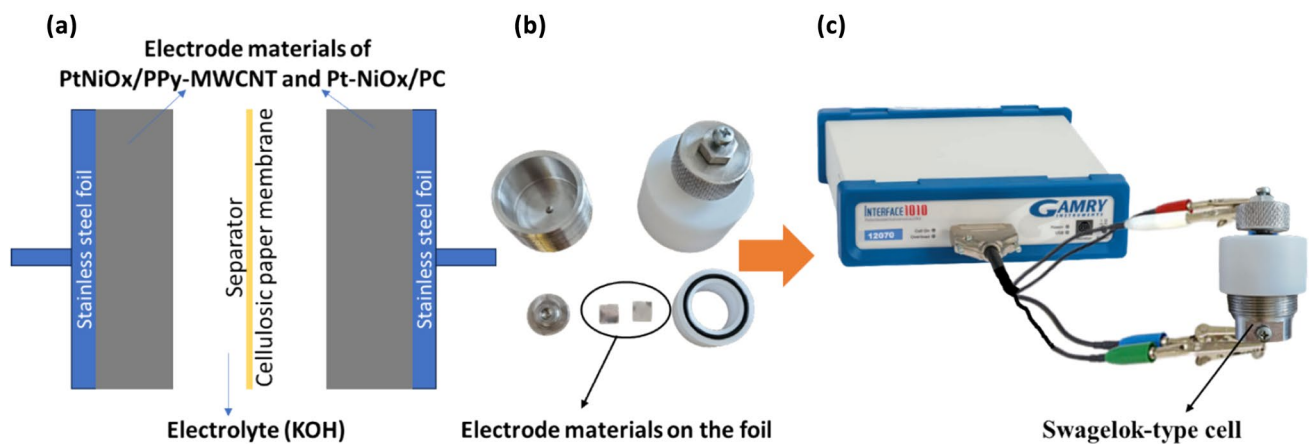


Fig. 3 **a** Schematic diagram of the capacitor, **b** image of the electrodes and inside of Swagelok-type cell, and **c** measurement system of capacitor

the mixture by vigorous stirring in 30 min. Finally, the obtained product was washed with plenty of distilled water and ethanol after centrifugation, and it was left to dry at 60 °C for 10 h [38].

2.5 Electrochemical measurements

The energy storage property analysis has been conducted with Swagelok-type cell and Gamry 1010-E galvanostat/potentiostat. In order to measure electrode properties, two equal amounts of Pt-NiO_x/PPy-MWCNT and Pt-NiO_x/PC as 0.36 g were dropped on the two same 1 cm diameter stainless-steel foils,

separately. After the electrode preparation, 6 M KOH aqueous solution has been prepared as electrolyte material. To prevent short-circuit of the cell, the cellulosic paper membrane was used between two electrodes. The capacitor diagram, image of the Swagelok-type cell and measurements system have been shown in Fig. 3a–c, respectively. The measurements were obtained for constant scan speeds of 100, 200, 400, and 800 mV/s. The CV measurements were conducted as 3 cycles to observe any anomalies, but only one CV cycle data were given in the result section to avoid data analysis confusion. In order to measure the capacitance, the two-electrode method was exploited.

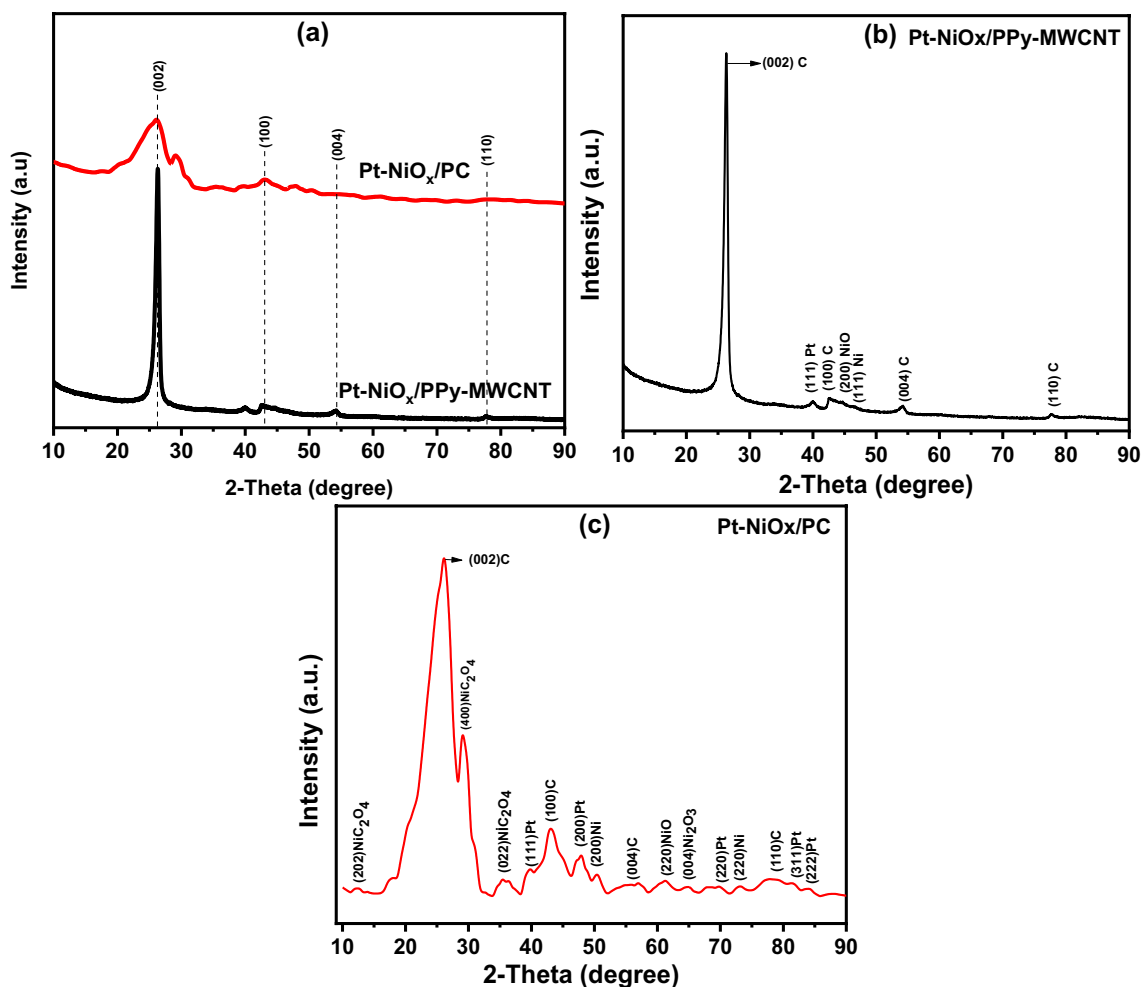


Fig. 4 XRD patterns of Pt-NiO_x/PPy-MWCNT and Pt-NiO_x/PC materials **a** all samples are together, **b** closer look XRD pattern of Pt-NiO_x/PPy-MWCNT and **c** Pt-NiO_x/PC

The cycle life study capacitance measurements were performed under 200 mV/s constant scanning speed in the range of 0–1 V for 200 cycles. Then, capacitance values of the samples were calculated with Eq. 1 in the reference of CV results [39].

$$C = \frac{\int IdV}{2m\Delta V\nu} \quad (1)$$

where I is current, m is the electrode active material weight as 0.36 g, ν is scan rate, and ΔV is voltage range.

2.6 Characterization

XRD measurements were carried out by a X-ray diffractometer (Rigaku Rint 1000) operating at Cu-K α radiation (40 kV, 40 mA). Surface analyzes of the materials were performed with scanning electron

microscopy (SEM) combined with energy dispersive spectroscopy (EDS) by ZEISS EVO18 SEM and Hitachi Regulus 8230 FE-SEM. Cyclic voltammetry (CV) electrochemical measurements were performed using Gamry Interface Potentiostat-Galvanostat (Gamry 1010E) instrument. Carbonization of *Astragalus brachycalyx* plant for PC material preparation was carried out in a nitrogen-bonded furnace by DEFNE Pyrolysis instruments.

3 Results and discussion

Figure 4 shows XRD pattern of the Pt-NiO_x/PPy-MWCNT and Pt-NiO_x/PC electrode materials for the range of 10–90° 2-Theta degrees. While the Fig. 4a indicates all the XRD patterns of the materials together, Fig. 4b and c show separately and closer look of the

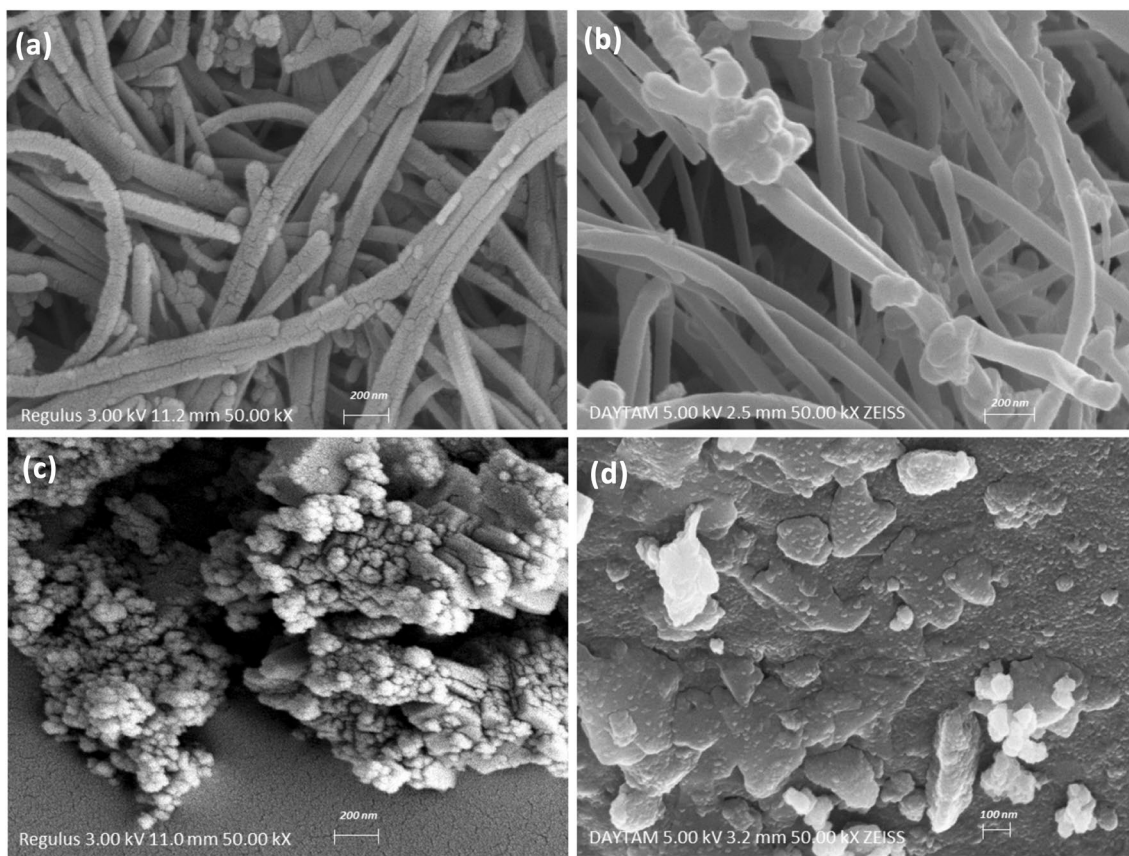


Fig. 5 SEM images of **a** MWCNT, **b** Pt-NiO_x/PPy-MWCNT, **c** PC and **d** Pt-NiO_x/PC materials

Pt-NiO_x/PPy-MWCNT and Pt-NiO_x/PC XRD patterns, respectively. Both Pt-NiO_x/PPy-MWCNT and Pt-NiO_x/PC exhibited XRD peaks due to having carbon composition according to Fig. 4a [40–42]. However, PC sample has more amorphous structure due to having non-sharp peaks. This result is in good agreement for PC samples according to literature [32]. Furthermore, the samples exhibited separately other peaks of their composition when the closer look in Fig. 4b and c. While the XRD patterns of the Pt-NiO_x/PPy-MWCNT exhibited Pt, Ni and NiO with carbon characteristic peaks, the Pt-NiO_x/PC revealed Pt, Ni, NiC₂O₄, Ni₂O₃ and NiO peaks in Fig. 4b and c according to JCPDS 04-0802 for platinum, JCPDS 04-0850 for nickel, JCPDS 25-0582 for NiC₂O₄, JCPDS 14-0481 for Ni₂O₃ and JCPDS 04-0835 NiO [43–47]. The phases of NiC₂O₄ and Ni₂O₃ compounds can be attributed to low synthesis temperature of the samples because calcinating temperature causes various phases of Ni and O elements [48, 49].

Figure 5a–d indicate SEM images of the MWCNT, PC, Pt-NiO_x/PPy-MWCNT and Pt-NiO_x/PC materials for 50.00 kx magnification scale, respectively. While

the MWCNT rods have been clearly identified in Fig. 5a and b, the PC has exhibited porous surfaces according to Fig. 5c and d. In the case of SEM images of Pt-NiO_x/PPy-MWCNT material in Fig. 5b, the supporting MWCNTs were coated or filled with related materials such as Ni, Pt, Pd and PPy, and the radii of rods are around 70–80 nm. These results are in good agreement with literature [50, 51]. In the case of SEM image of the Pt-NiO_x/PC, the porous structures in Fig. 5d can be seen with big blocks which have 200 nm to 1–2 μm sizes, and structures are homogeneously distributed.

Figure 6a and b show EDS analysis results of the Pt-NiO_x/PPy-MWCNT and Pt-NiO_x/PC materials, respectively. All materials have exhibited C and O peaks due to having porous carbon and MWCNT in the composition as well as NiO_x compounds. Atomic and weight ratios also have been given in the inset of Fig. 6a and b. The results clearly revealed that the amount of the elements was almost protected.

CV analyses were performed to determine electrochemical characteristics of Pt-NiO_x/PPy-MWCNT and Pt-NiO_x/PC electrode materials before analyzing

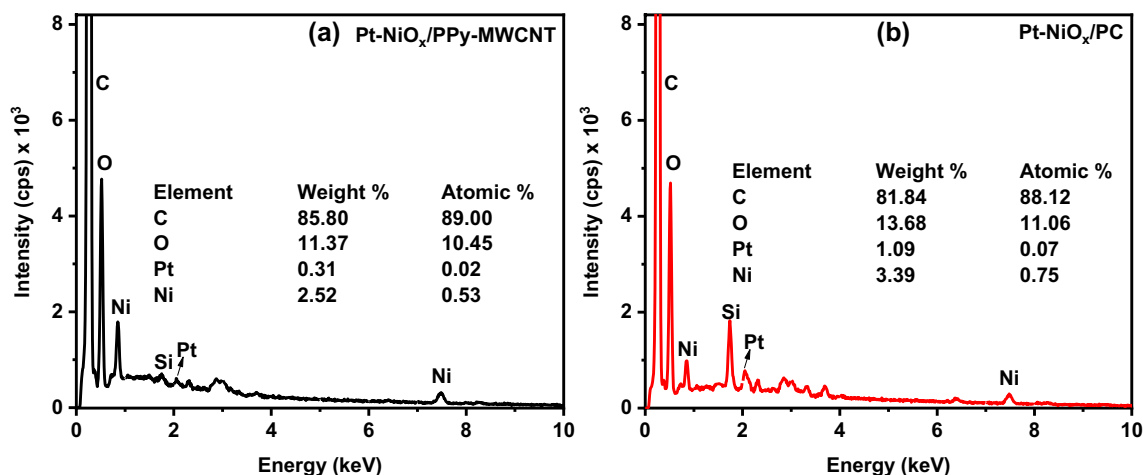


Fig. 6 EDS spectrum of **a** Pt-NiO_x/PPy-MWCNT and **b** Pt-NiO_x/PC

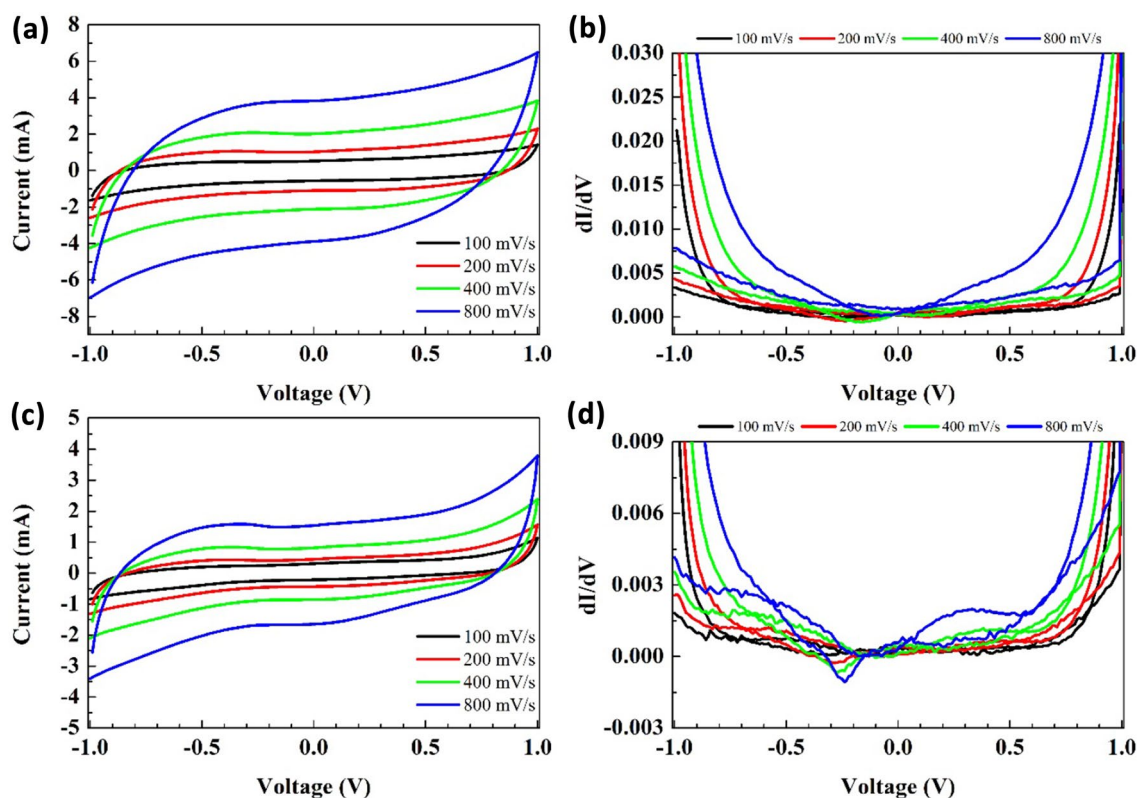


Fig. 7 CV analysis of Pt-NiO_x/PPy-MWCNT and Pt-NiO_x/PC electrodes. **a** V of Pt-NiO_x/PPy-MWCNT, **b** dI/dV of Pt-NiO_x/PPy-MWCNT, **c** CV of Pt-NiO_x/PC, **d** dI/dV of Pt-NiO_x/PC

the operating performance in energy storage systems. Figure 7a–d shows the CV and dI/dV analyzes of the Pt-NiO_x/PPy-MWCNT (Fig. 7a and b) and Pt-NiO_x/PC (Fig. 7c and d) samples. As seen in the Fig. 7a, almost rectangular shape current characteristic was obtained

for CV characteristics of the Pt-NiO_x/PPy-MWCNT. This shows that the MWCNT structure exhibits electric double-layer capacitor (EDLC) feature [52]. On the other hand, in Pt-NiO_x/PC (Fig. 7c) electrode material exhibited some Faradaic reactions and degradations

in the rectangular CV characteristic. However, these Faradaic reactions can be thought to have weak pseudocapacitive effects that do not suppress the EDLC characteristic. This situation especially reveals the difference in capacitive effect between Pt-NiO_x/PPy-MWCNT and Pt-NiO_x/PC electrode materials. Furthermore, dI/dV analyzes were also performed using CV results to display the analysis of possible redox reactions. The Pt-NiO_x/PPy-MWCNT electrode material has rectangular shape CV characteristics, and there is no determined redox reaction in the range of ± 1 V or the samples show permanent capacitive current plateaus in the range of ± 1 V. Moreover, these capacitive current plateaus generally resemble characteristic supercapacitor current plateaus [53, 54]. This situation shows that the Pt-NiO_x/PPy-MWCNT electrode material may store energy at high level capacitance values as a supercapacitor. In addition, another important point is that the Pt-NiO_x/PPy-MWCNT electrode material shows an increasing capacitive current trend when the value of scanning speed increase from 100 mV/s to 800 mV/s. This reveals that Pt-NiO_x/PPy-MWCNT electrode material has fast charge discharge the energy behavior.

According to CV characteristic of Pt-NiO_x/PC electrode material (Fig. 7c), some redox reactions occurred in the structure depending on the increased voltage scanning rate, and the rectangular shape CV feature revealed. According to literature research, these redox peaks occur due to the Ni²⁺/Ni³⁺ transitions in the 0–0.50 V region, and it is caused especially by the OH⁻ ion from the KOH_(aq) electrolyte [55]. While there are NiO and Ni₂O₃ phases that can provide these transitions in the Pt-NiO_x/PC, the effect of NiC₂O₄ (another phase in the structure) was also investigated based on the literature. In the study of Sahu et al. in 2021, the NiC₂O₄ phase had only a capacitive effect [56]. On the other hand, when the CV values of study by Sahu et al. were compared with CV of Pt-NiO_x/PC, it was determined that the Pt-NiO_x/PC electrode material provided approximately 100 times lower current value (Sahu et al. obtained ~ 0.12 A at 0.40 V and 100 mV/s scan rate). This shows that the presence of NiC₂O₄ in the Pt-NiO_x/PC structure is at a negligible level. In addition, when the dI/dV are examined, the anodic and cathodic peak voltage levels reducing depending on increasing scan speeds. Pt-NiO_x/PC electrode material has anodic peaks at 0.35, 0.32, 0.30, and 0.28 V

and cathodic peaks at 0.40, 0.38, 0.35, and 0.32 V for 100, 200, 400, and 800 mV/s scan speeds, respectively. This show that the material can adapt to high-speed charge-discharge energy storage processes. The most important factor in this situation is that the Pt elements in the electrodes increase the structural stabilization [57]. Because, within the transition metal group, elements such as Ni (58.69 u), Mn (54.94 u) and Co (58.93 u) are generally most used metal elements in energy storage systems. Compared to these, the Pt (195.08 u) element has a higher atomic weight [58]. This can be thought as an important factor for reducing the mechanical vibrations occurring in molecular and crystal structures, especially during the insertion/disinsertion processes of ions into electrodes.

The first charge-discharge capacitance values, the first-3 discharge capacitance values under various scanning speeds and 200 cycle cycle-life analysis have been displayed in Fig. 8a–d for Pt-NiO_x/PPy-MWCNT and Pt-NiO_x/PC electrode materials. The data shown in Fig. 8a, c and d belong to a scan rate of 200 mV/s. The most important factor for presenting the data obtained at a scanning speed of 200 mV/s is to obtain higher scanning speed than other analyzes performed in the literature. Since circuit components operating at higher speeds have been demanded in technological applications, we have desired to show the characteristic behaviors more clearly by that way. The Pt-NiO_x/PPy-MWCNT and Pt-NiO_x/PC have 252.36 F/g and 390.97 F/g charge capacitance values, respectively. The discharge capacitance values obtained as 199.82 F/g and 230.89 F/g for Pt-NiO_x/PPy-MWCNT and Pt-NiO_x/PC, respectively. The results highlighted that both of two electrode materials show supercapacitor feature. Moreover, the Pt-NiO_x/PC electrode material shows an anomaly according to charge-discharge capacitance differences. There is a capacity loss of about 35% between the stored energy and the discharged energy for first cycle.

Figure 8b shows the analysis of the specific capacitances of the first three cycles depending on 100–800 mV/s scanning speeds for Pt-NiO_x/PPy-MWCNT and Pt-NiO_x/PC electrode materials. The most important indicator of this analysis is the change in the stored energy depending on the increasing scanning speed. For a more detailed analysis of stored energy changes, the capacity retention calculations were obtained for the first 3 discharge cycles for 100–800 mV/s scan rates.

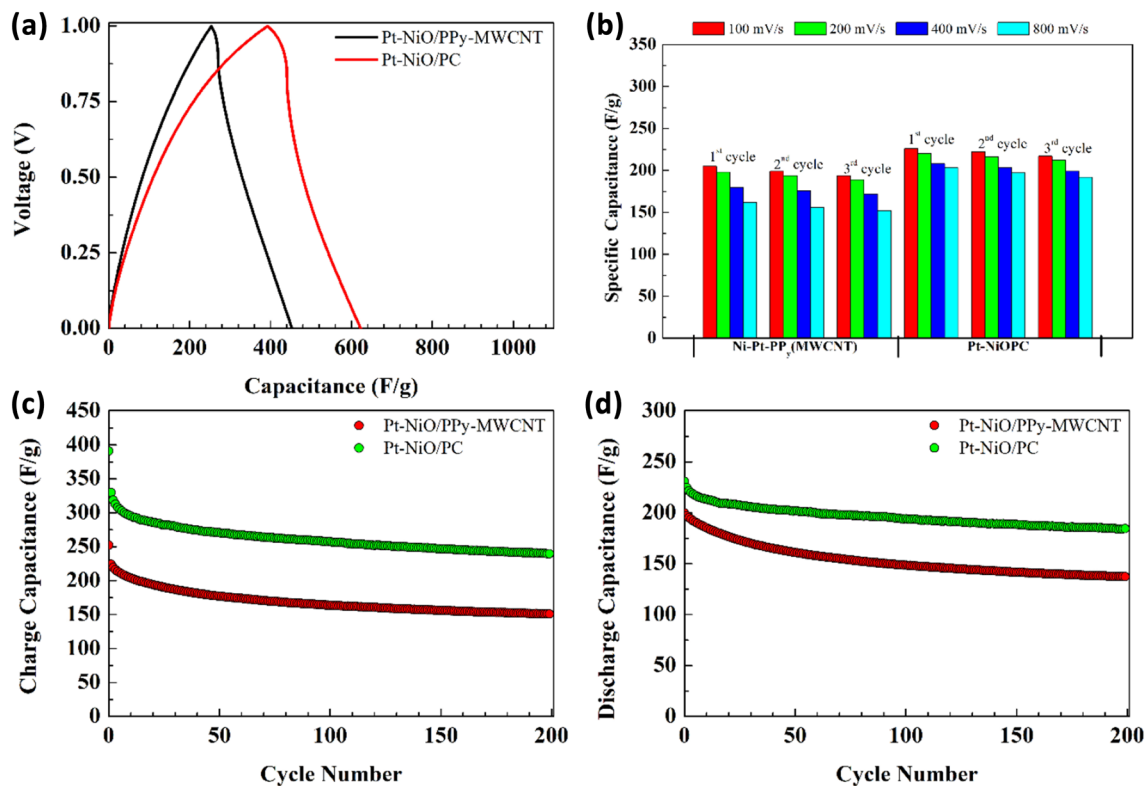


Fig. 8 **a** First charge-discharge characteristics capacitors, **b** first-3 cycles specific capacitance behaviors depending on different scan rates, **c** charge capacitance behaviors, **d** discharge capacitance behaviors of Pt-NiO_x/PPy-MWCNT and Pt-NiO_x/PC

Table 1 Discharge capacitance retention values depending on scan rate for first 3 cycles

Scan rate (mV/s)	Pt-NiO _x /PPy-MWCNT				Pt-NiO _x /PC			
	1st (F/g)	2nd (F/g)	3th (F/g)	CR (%)	1st (F/g)	2nd (F/g)	3th (F/g)	CR (%)
100	203	200	198	97.60	223	220	217	97.40
200	199	197	195	98	230	224	221	96.10
400	179	177	175	97.80	220	213	210	95.50
800	163	161	160	98.20	207	202	199	96.10

Capacity retention (CR) values are calculated as given by following formula:

$$CR = \frac{C_0 - C_n}{C_0}, \tag{2}$$

where C₀ is the first-cycle capacitance value (F/g) and C_n is the last cycle capacitance value (F/g). Capacitance and CR values depending on scanning speeds during 3 cycles are given in Table 1 for comparison. When the differences in CR performances were examined together with the morphological features, it was determined that the Pt-NiO_x/PPy-MWCNT electrode material responded better to K⁺ or OH⁻ polarization

than the Pt-NiO_x/PC electrode material with their porous structure. Therefore, both electrode materials have more stable CR performance in charge-discharge processes at high speeds.

The cycle-life analysis of the Pt-NiO_x/PPy-MWCNT and Pt-NiO_x/PC have been indicated in Fig. 8c and d for charging and discharging, respectively. Similar to the results of Fig. 8a, the charge-discharge capacitance difference of the Pt-NiO_x/PC electrode material is clearly seen. However, although there is a difference in charge-discharge capacitance compared to other materials, Pt-NiO_x/PC provides more stable energy for discharge capacitance stability. That is, the

Table 2 The capacitance values of some specific cycles and capacitance retention values

Sample	1. cycle		50. cycle		100. cycle		200. cycle		CR (%)	
	Ch.	Dch.	Ch.	Dch.	Ch.	Dch.	Ch.	Dch.	Ch.	Dch.
Pt-NiO/PPy-MWCNT	252.36	199.82	177.57	161.38	163.98	148.71	151.18	137.37	59.90	68.80
Pt-NiO/PC	390.96	230.89	270.89	201.66	257.29	194.08	239.75	184.52	61.30	79.90

Table 3 Capacitive performance comparison of carbon-type electrode materials

Electrode Material	Type	Specific Capacitance (F/g)	Capacity Retention (%)	References
Vertical Graphene Nanosheets	Graphene-based	230	> 99	[59]
N-Graphene	Graphene-based	405	87.70	[60]
NiSe on Graphene	Graphene-based	1280	98	[61]
Three Rose Petal-Derived Porous Carbons	Carbon-based	56	–	[62]
TiC-Derived Nanoporous Carbon	Carbon-based	163	107	[63]
Multiwalled Carbon Nanotube	MWCNT-based	32–41	–	[64]
LiNi _{0.8} Co _{0.2} O ₂ /MWCNT	MWCNT-based	196.70	54.20	[65]
Multiwalled Carbon Nanotube	MWCNT-based	18.50	–	[65]
Pt-NiO/PPy-MWCNT	MWCNT-based	199.82	68.80	This Study
Pt-NiO/PC	Carbon-based	230.89	79.90	This Study

Pt-NiO/PC material is structurally more stable state. On the other hand, Pt-NiO_x/PPy-MWCNT capacitance values decreased during the increasing cycles. In order to analyze this situation better and to determine which material exhibits more stable performance, the CR values are calculated for 200 cycles (at 200 mV/s scan rate) and given in Table 2. The contribution of Pt to the structural stability (for Pt-NiO_x/PC electrode material) during 200 cycles shows that oxidative reactions are sustained in longer cycles than other samples. Although the Pt-NiO_x/PC has disadvantageous at high speeds charge-discharge, the Pt stabilization creates a great advantage especially for porous structure than other samples.

When evaluations are made in terms of technology and industrial uses, commercial MWCNT with PPy and green synthesized PC have great importance, especially for this study because it is of great importance to use both economical and environmentally friendly materials in energy storage systems to produce alternatives to expensive nanotubes. However, this makes it difficult to achieve the desired high capacitive performances. For this reason, it is aimed to increase the capacitive performance by loading Pt and NiO into our economical and environmentally friendly materials. Whether this aim has been achieved

Table 4 Comparison of Pt-NiO_x/PPy-MWCNT and Pt-NiO_x/PC supercapacitors for industrial applications

Sample	Capacitance	CR rate	Energy storage stability
Pt-NiO/PPy-MWCNT	Good	Good	Good
Pt-NiO/PC	Better	Better	Better

or not is revealed by a literature comparison shown in Table 3.

The capacitive performances and CR values of carbon-based materials given in Table 3. It has been determined that Pt-NiO_x/PC and Pt-NiO_x/PPy-MWCNT materials offer higher capacitive performance and CR values than many other carbon-derived electrodes. This situation also supports the application comparison given in Table 4. When a general evaluation is made, it is thought that Pt-NiO_x/PC and Pt-NiO_x/PPy-MWCNT will be more economical and more environmentally friendly alternative materials for energy storage systems.

Capacitive performance results of Pt-NiO_x/PPy-MWCNT and Pt-NiO_x/PC supercapacitors have been listed in Table 4 for the classification of good and better

in terms of use in industry and technology. In this comparison, the first charge-discharge performances, the first 3 cycles of discharge capacitance values at various scanning speeds, the 200-cycle cycle-life results at a constant scanning speed of 200 mV/s, CR calculation values and data in Table 3 for these results were taken into account. In this context, it has been determined that Pt-NiO_x/PC is better than Pt-NiO_x/PPy-MWCNT. Moreover, it is considered that both materials have high capacitance values at levels that can be used in industry.

4 Conclusion

We prepared Pt-NiO_x/PPy-MWCNT and Pt-NiO_x/PC materials by a facile synthesis method for supercapacitor electrode materials to usage in technological applications. The electrode materials were characterized by XRD, SEM and EDS analyses. The XRD results revealed crystalline structure of the composition of the related materials such as C, Pt, Ni in the electrodes. SEM images of the materials confirmed filled rod like and porous surfaces of the MWCNT and PC supported materials. EDS analysis approved chemical composition of the Pt-NiO_x/PPy-MWCNT and Pt-NiO_x/PC depending on their ingredients. The capacitance values of the Pt-NiO_x/PPy-MWCNT and Pt-NiO_x/PC materials were obtained as 252.36 and 390.97 F/g, respectively. The comparison of the materials was made according CR and energy storage stability. As a results, the synthesized electrode materials can be used for supercapacitor applications.

Author contributions

SD: contributed to investigation, methodology, data curation and writing original draft. MSN: contributed to investigation, synthesis and methodology. AK: contributed to writing—reviewing and editing. MHÇ: contributed to investigation, synthesis, methodology and writing original draft. MHA: contributed to writing—reviewing and editing.

Funding

Open access funding provided by the Scientific and Technological Research Council of Türkiye (TÜBİTAK). The authors are grateful to the Iğdır University Research laboratory and Research Center (ALUM) for providing of pyrolysis device.

Data availability

Data will be available upon reasonable request.

Declarations

Conflict of interest The authors declare that they have no conflict of interest.

Open Access This article is licensed under a Creative Commons Attribution 4.0 International License, which permits use, sharing, adaptation, distribution and reproduction in any medium or format, as long as you give appropriate credit to the original author(s) and the source, provide a link to the Creative Commons licence, and indicate if changes were made. The images or other third party material in this article are included in the article's Creative Commons licence, unless indicated otherwise in a credit line to the material. If material is not included in the article's Creative Commons licence and your intended use is not permitted by statutory regulation or exceeds the permitted use, you will need to obtain permission directly from the copyright holder. To view a copy of this licence, visit <http://creativecommons.org/licenses/by/4.0/>.

References

1. M. Sevilla, R. Mokaya, *Energy Environ. Sci.* **7**, 1250–1280 (2014)
2. J. Castro-Gutiérrez, A. Celzard, V. Fierro, *Front. Mater.* **7**, 217 (2020)
3. A. Riaz, M.R. Sarker, M.H.M. Saad, R. Mohamed, *Sensors* **21**, 5041 (2021)
4. W. Zhang, W. Yang, H. Zhou, Z. Zhang, M. Zhao, Q. Liu, J. Yang, X. Lu, *Electrochim. Acta.* **357**, 136855 (2020)
5. B.K. Kim, S. Sy, A. Yu, J. Zhang, *Handbook of clean energy systems* (Wiley, Hoboken, 2015), pp.1–25
6. S. Huang, X. Zhu, S. Sarkar, Y. Zhao, *APL Mater.* **7**, 100901 (2019)
7. J. Liu, G. Cao, Z. Yang, D. Wang, D. Dubois, X. Zhou, G.L. Graff, L.R. Pederson, J.G. Zhang, *ChemSusChem* **1**, 676 (2008)
8. M.E. Şahin, F. Blaabjerg, A. Sangwongwanich, *Energies* (Basel). **15**, 674 (2022)
9. K.C.S. Lakshmi, B. Vedhanarayanan, *Batteries.* **9**, 202 (2023)

10. P. Forouzandeh, V. Kumaravel, S.C. Pillai, *Catalysts*. **10**, 969 (2020)
11. A.K. Sharma, Y. Sharma, R. Malhotra, J.K. Sharma, *Adv. Mat. Lett.* **3**, 82 (2012)
12. K.Y.T. Lee, H.H. Shi, K. Lian, H.E. Naguib, *Smart Mater. Struct.* **24**, 115008 (2015)
13. S. Yu, V.M.H. Ng, F. Wang, Z. Xiao, C. Li, L.B. Kong, W. Que, K. Zhou, *J. Mater. Chem. A*. **6**, 9332 (2018)
14. M. Krajewski, P.Y. Liao, M. Michalska, M. Tokarczyk, J.Y. Lin, *J. Energy Storage*. **26**, 101020 (2019)
15. Y. Zhu, S. Murali, M.D. Stoller, K.J. Ganesh, W. Cai, P.J. Ferreira, A. Pirkle, R.M. Wallace, K.A. Cychosz, M. Thommes, D. Su, E.A. Stach, R.S. Ruoff, *Science* **332**, 1537 (1979)
16. X. Chen, R. Paul, L. Dai, *Natl. Sci. Rev.* **4**, 453 (2017)
17. K.J. Huang, L. Wang, Y.J. Liu, H.B. Wang, Y.M. Liu, L.L. Wang, *Electrochim. Acta*. **109**, 587 (2013)
18. J. Jiang, J. Zhu, Y. Feng, J. Liu, X. Huang, *Chem. Commun.* **48**, 7471 (2012)
19. F. Wang, X. Zhan, Z. Cheng, Z. Wang, Q. Wang, K. Xu, M. Safdar, J. He, *Small*. **11**, 749 (2015)
20. J. Jose, J. Vigneshwaran, A. Baby, R. Viswanathan, S.P. Jose, and S. P B, *J Alloys Compd.* **896**, 163067 (2022)
21. C.O. Chikere, N.H. Faisal, P. Kong-Thoo-Lin, C. Fernandez, *Nanomaterials* **10**, 537 (2020)
22. Z. Liu, S. Zhang, L. Wang, T. Wei, Z. Qiu, Z. Fan, *Nano Select.* **1**, 244 (2020)
23. Y. Yin, G. Cao, L. Fu, Z. Wei, H. Li, P. Wu, M. Li, H. Zong, L. Yan, B. Zhang, *J. Alloys Compd.* **854**, 157016 (2021)
24. C. Wang, H. Zhang, C. Feng, S. Gao, N. Shang, Z. Wang, *Catal. Commun.* **72**, 29 (2015)
25. Z. Wang, C. Xu, G. Gao, X. Li, *RSC Adv.* **4**, 13644 (2014)
26. L. Que, L. Zhang, C. Wu, Y. Zhang, C. Pei, F. Nie, *Carbon* **145**, 281 (2019)
27. J. Chen, T. Ma, M. Chen, Z. Peng, Z. Feng, C. Pan, H. Zou, W. Yang, S. Chen, *J. Energy Storage*. **32**, 101895 (2020)
28. B.S. Singu, K.R. Yoon, *Electrochim. Acta*. **268**, 304 (2018)
29. K.S. Bhavani, T. Anusha, P.K. Brahman, *Electrochim. Acta*. **399**, 139394 (2021)
30. R. Atchudan, T.N.J.I. Edison, S. Perumal, P. Thirukumar, R. Vinodh, Y.R. Lee, *J. Taiwan. Inst. Chem. Eng.* **102**, 475 (2019)
31. Z. Xu, X. Zhang, Y. Liang, H. Lin, S. Zhang, J. Liu, C. Jin, U. Choe, K. Sheng, *Energy Fuels* **34**, 8966 (2020)
32. L. Guan, L. Pan, T. Peng, C. Gao, W. Zhao, Z. Yang, H. Hu, M. Wu, *ACS Sustain. Chem. Eng.* **7**, 8405 (2019)
33. D. Gandla, X. Wu, F. Zhang, C. Wu, D.Q. Tan, *ACS Omega*. **6**, 7615 (2021)
34. J. Zhao, Y. Cui, J. Zhang, J. Wu, Y. Yue, G. Qian, *Ind. Eng. Chem. Res.* **60**, 11637 (2021)
35. H. Demiral, C. Güngör, *J. Clean. Prod.* **124**, 103 (2016)
36. T.M. Wu, H.L. Chang, Y.W. Lin, *Compos. Sci. Technol.* **69**, 639 (2009)
37. P.C. Ramamurthy, A.M. Malshe, W.R. Harrell, R.V. Gregory, K. McGuire, A.M. Rao, *Solid State Electron.* **48**, 2019 (2004)
38. M. Köktürk, F. Altındag, M.S. Nas, M.H. Calimli, *Biol. Trace Elem. Res.* **200**, 2455 (2021)
39. K. Cicek, S. Demirel, *J. Mater. Sci.: Mater. Electron.* **32**, 16335 (2021)
40. P. Nie, C. Min, H.J. Song, X. Chen, Z. Zhang, K. Zhao, *Tribol Lett.* **58**, 1 (2015)
41. G. An, P. Yu, M. Xiao, Z. Liu, Z. Miao, K. Ding, L. Mao, *Nanotechnology*. **19**, 275709 (2008)
42. R. Atchudan, A. Pandurangan, J. Joo, *J. Nanosci. Nanotechnol.* **15**, 4255 (2015)
43. M.A. Shah, *Scientia Iranica*. **19**, 964 (2012)
44. B. Li, C. Li, Y. Gao, H. Guo, Y. Kang, S. Zhao, *Coatings*. **9**, 822 (2019)
45. J.F. Gao, D.L. Fang, Z.B. Wang, P.H. Yang, C.S. Chen, *Sens. Actuators A Phys.* **135**, 472 (2007)
46. Z. Wei, H. Qiao, H. Yang, C. Zhang, X. Yan, *J. Alloys Compd.* **479**, 855 (2009)
47. S. Dey, S. Santra, A. Midya, P.K. Guha, S.K. Ray, *Environ. Sci. Nano.* **4**, 191 (2017)
48. S. Rakshit, S. Ghosh, S. Chall, S.S. Mati, S.P. Moulik, S.C. Bhattacharya, *RSC Adv.* **3**, 19348 (2013)
49. H. Long, T. Shi, H. Hu, S. Jiang, S. Xi, Z. Tang, *Sci. Rep.* **4**, 1 (2014)
50. P.Y. Zhao, H.Y. Wang, G.S. Wang, *Front. Chem.* **8**, 97 (2020)
51. M. Kozłowski, E. Czerwosz, K. Sobczak, *Photonics Appl. Astron. Commun. Ind. High Energy Phys. Exp.* **11581**, 1044553 (2017)
52. S. Hasumi, S. Iwakami, Y. Sasaki, S. Faraezi, M.S. Khan, T. Ohba, *Batteries* **9**, 212 (2023)
53. Y. Han, X. Chen, W. Yue, A. Huang, *MRS Commun.* **12**, 238–244 (2022)
54. D. Khalafallah, M. Zhi, Z. Hong, *J. Colloid Interface Sci.* **606**, 1352 (2022)
55. S. Wu, K.S. Hui, K.N. Hui, J.M. Yun, K.H. Kim, *RSC Adv.* **7**, 41771 (2017)
56. K.K. Sahu, R.K. Sahoo, L.D. Beshra, M. Mohapatra, *Ionics (Kiel)*. **27**, 819 (2021)
57. Q. Cheng, S. Yang, C. Fu, L. Zou, Z. Zou, Z. Jiang, J. Zhang, H. Yang, *Energy Environ. Sci.* **15**, 278 (2022)
58. M.S. Park, J. Kim, K.J. Kim, J.W. Lee, J.H. Kim, Y. Yamauchi, *Phys. Chem. Chem. Phys.* **17**, 30963 (2015)

59. D. Han Seo, Z. Jun Han, S. Kumar, K. Ostrikov, D.H. Seo, Z.J. Han, S. Kumar, K. Ostrikov, *Adv. Energy Mater.* **3**, 1316 (2013)
60. N.A. Elessawy, J.E. Nady, W. Wazeer, A.B. Kashyout, *Sci. Rep.* **2019**, *9*(19), 1 (2019)
61. B. Kirubasankar, V. Murugadoss, J. Lin, T. Ding, M. Dong, H. Liu, J. Zhang, T. Li, N. Wang, Z. Guo, S. Angaiah, *Nanoscale*. **10**, 20414 (2018)
62. S.W. Xu, M.C. Zhang, G.Q. Zhang, J.H. Liu, X.Z. Liu, X. Zhang, D.D. Zhao, C.L. Xu, Y.Q. Zhao, *J. Power Sources*. **441**, 227220 (2019)
63. M. Käärrik, M. Arulepp, J. Kozlova, J. Aruväli, U. Mäeorg, A. Kikas, V. Kisand, A. Tamm, J. Leis, *J. Solid State Electrochem.* **26**, 2365 (2022)
64. G.P. Pandey, S.A. Hashmi, Y. Kumar, *J. Electrochem. Soc.* **157**, A105 (2010)
65. G. Wang, M. Qu, Z. Yu, R. Yuan, *Mater. Chem. Phys.* **105**, 169 (2007)

Publisher's Note Springer Nature remains neutral with regard to jurisdictional claims in published maps and institutional affiliations.